Electronic Supplementary Information

Light-up covalent organic frameworks via the flexible walls design for chemical sensing

Wanyi Zhao,[a] Ce Xing,[a] Yuwei Zhang,*[a] Juntao Ren*[b] and He Li*[b]

[a] Laboratory of Preparation and Applications of Environmental Friendly Materials (Jilin Normal University), Ministry of Education, Changchun, 130103, China, E-mail: yw_zhang@jlnu.edu.cn.

[b] Division of Energy Materials, Dalian Institute of Chemical Physics, Chinese Academy of Sciences, Dalian 116023, China, E-mail: jtren@dicp.ac.cn; lihe@dicp.ac.cn.

Materials

Acetic acid, tetrahydrofuran, n-butanol, o-DCB, DMF, and other chemicals were obtained from J&K Scientific company, TCI, Wako, and Sigma-Aldrich. 4,4',4''-((1,3,5-triazine-2,4,6-triyl)tris(oxy))trianiline (TTTTA), 3-hydroxy-[1,1'-biphenyl]-4,4'-dicarbaldehyde (BP-OH-1), and 3,3'-dihydroxy-[1,1'-biphenyl]-4,4'-dicarbaldehyde (BP-OH-2) were purchased form Jilin Chinese Academy of Sciences - Yanshen Technology Co., Ltd.

Characterization

Fourier transform infrared (FT-IR) spectra were recorded on a JASCO model FT IR-6100 infrared spectrometer. X-ray diffraction (XRD) data were recorded on a Bruker D8 Focus Powder X-ray Diffractometer by using powder on glass substrate, from 2θ = 1.5° up to 30° with 0.02° increment. Solid-state NMR spectra were obtained with a Bruker 500 MHz spectrometer equipped with a magic-angle spin probe using a 4 mm ZrO_2 rotor. Nitrogen sorption isotherms were measured at 77 K with a TriStar II instrument (Micromeritics). The Brunauer-Emmett-Teller (BET) method was utilized to calculate the specific surface areas. By using the non-local density functional theory (NLDFT) model, the pore volume was derived from the sorption curve. The fluorescence spectra were collected at room temperature using the Hitachi F-700 spectrophotometer. EDS Elemental analysis was performed on a Euro Vector EA3000 elemental analyzer. Field-emission scanning electron microscopy (FE-SEM) images were performed on a JEOL model JSM-6700 operating at an accelerating voltage of 5.0 kV. The samples were prepared for SEM by drop-casting a tetrahydrofuran suspension onto mica substrate and then coated with gold.

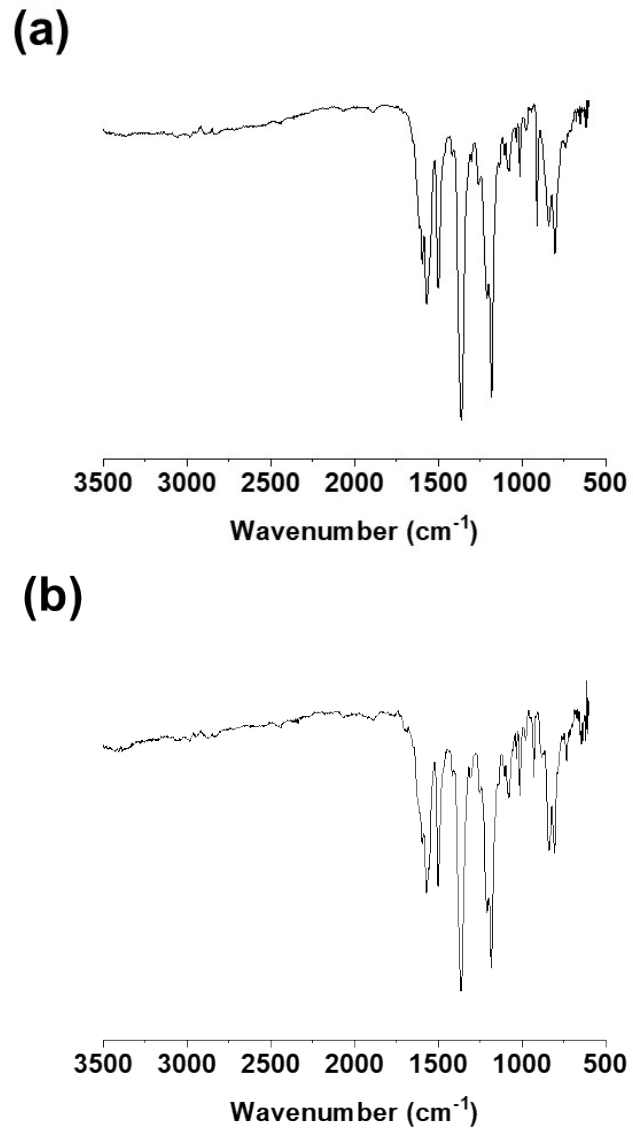

Fig. S1 FT-IR spectra of (a) TTTT-COF-1 and (b) TTTT-COF-2.

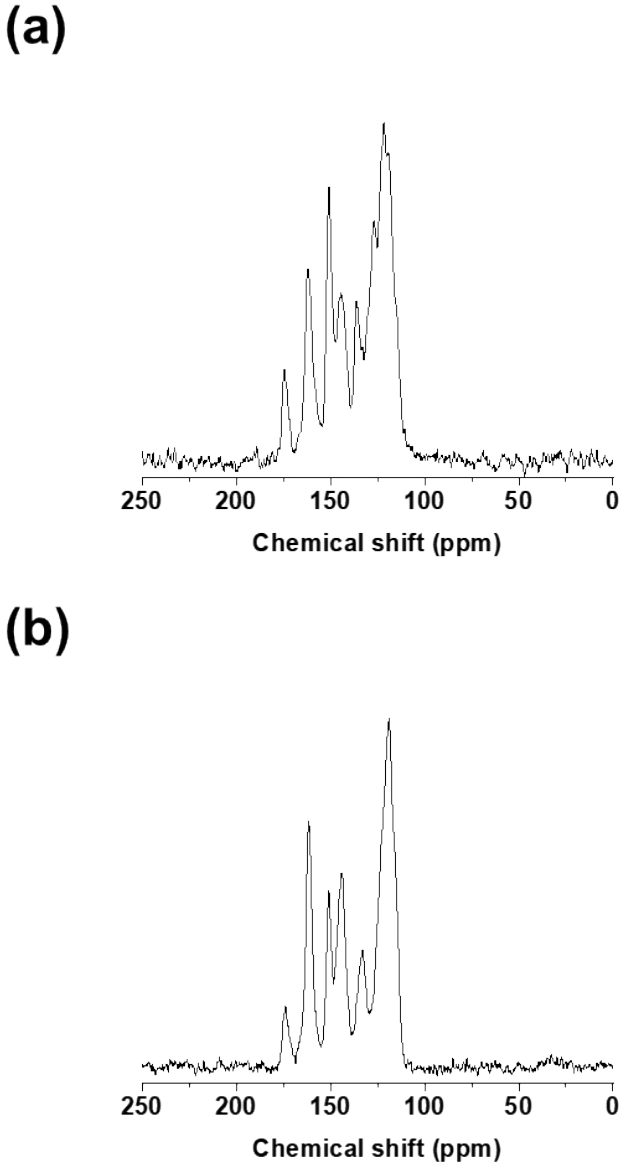

Fig. S2 Solid ^{13}C NMR spectra of (a) TTTT-COF-1 and (b) TTTT-COF-2.

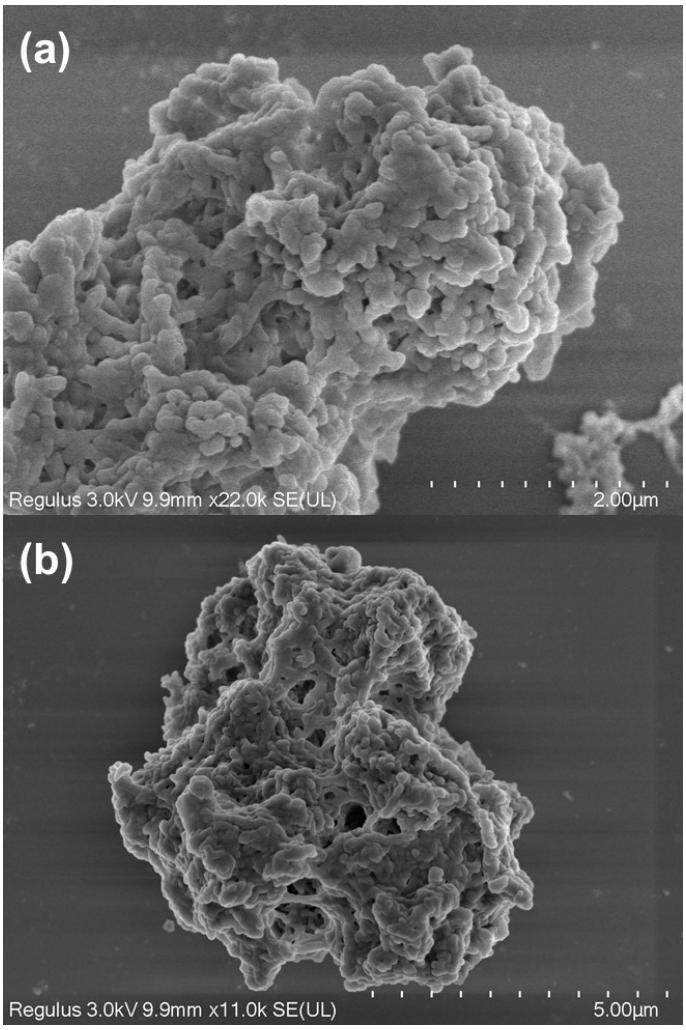

Fig. S3 FE SEM images of (a) TTTT-COF-1 and (b) TTTT-COF-2.

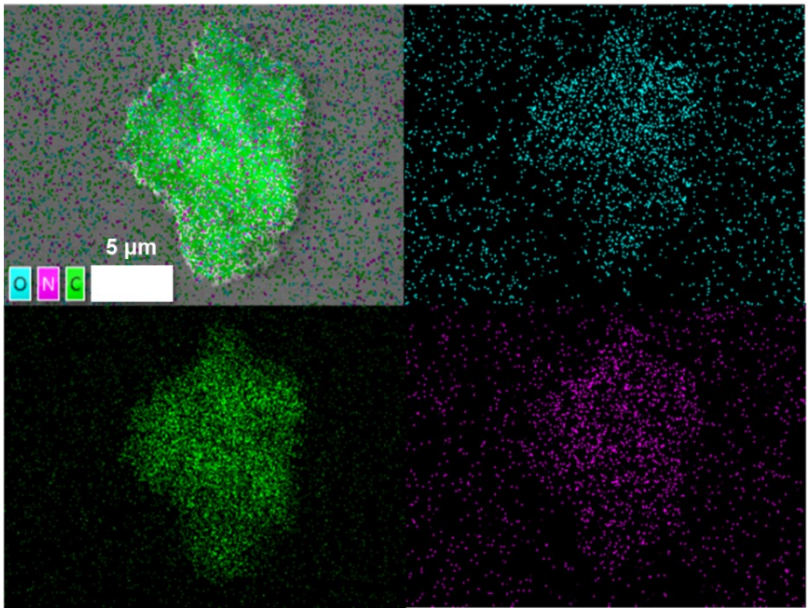

Fig. S4 EDS mapping images of TTTT-COF-1.

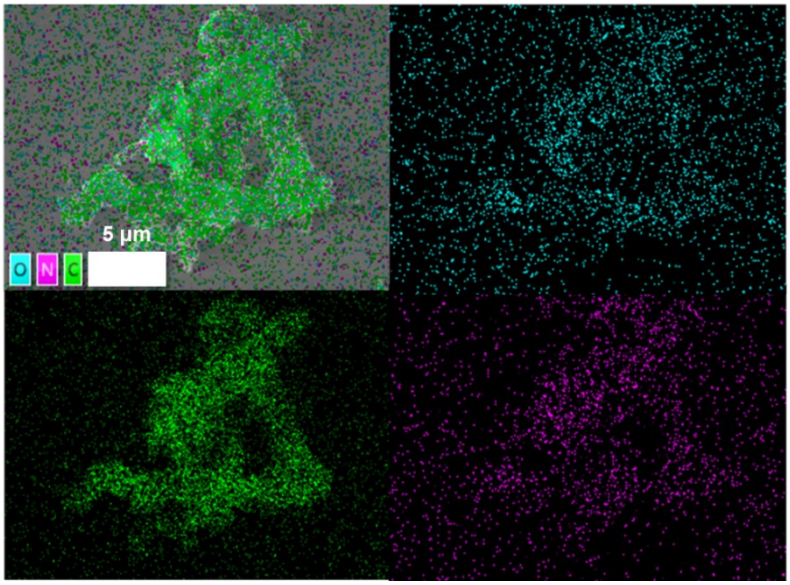

Fig. S5 EDS mapping images of TTTT-COF-2.

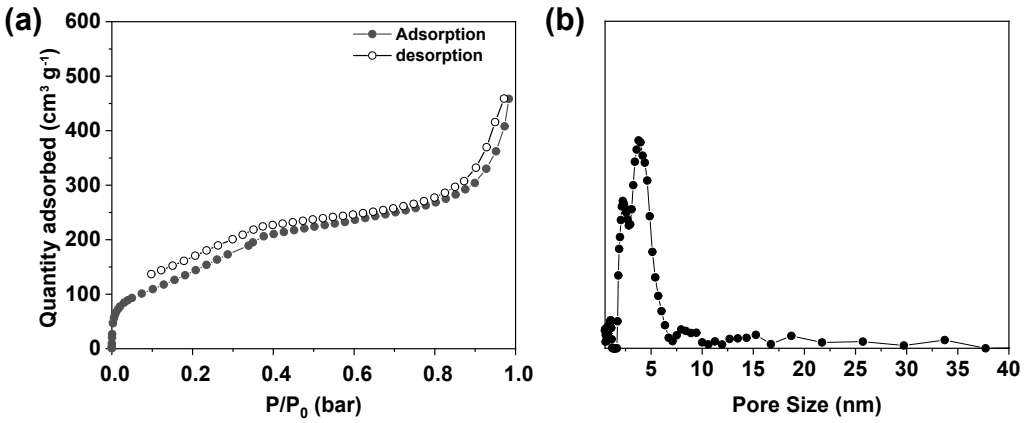

Fig. S6 (a) Nitrogen adsorption-desorption isotherms of TTTT-COF-1 measured at 77 K. (b) Pore size distribution of TTTT-COF-1.

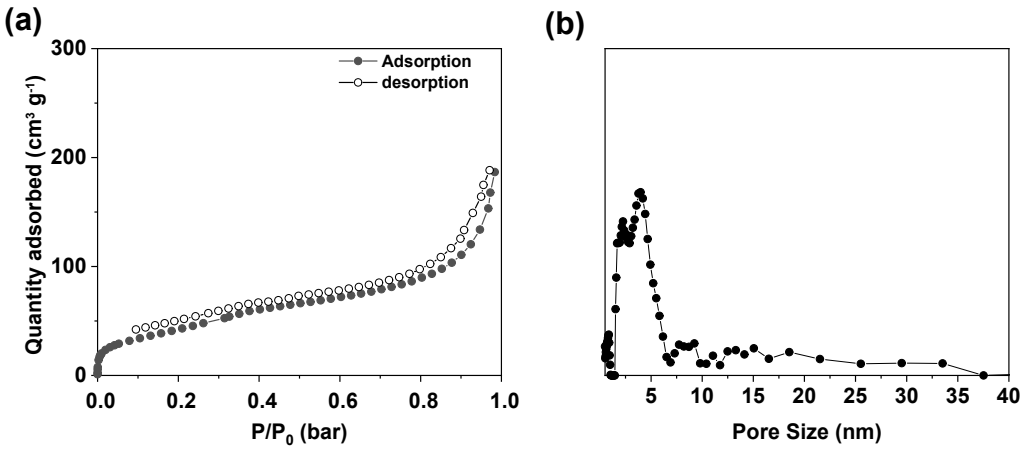

Fig. S7 (a) Nitrogen adsorption-desorption isotherms of TTTT-COF-2 measured at 77 K. (b) Pore size distribution of TTTT-COF-2.

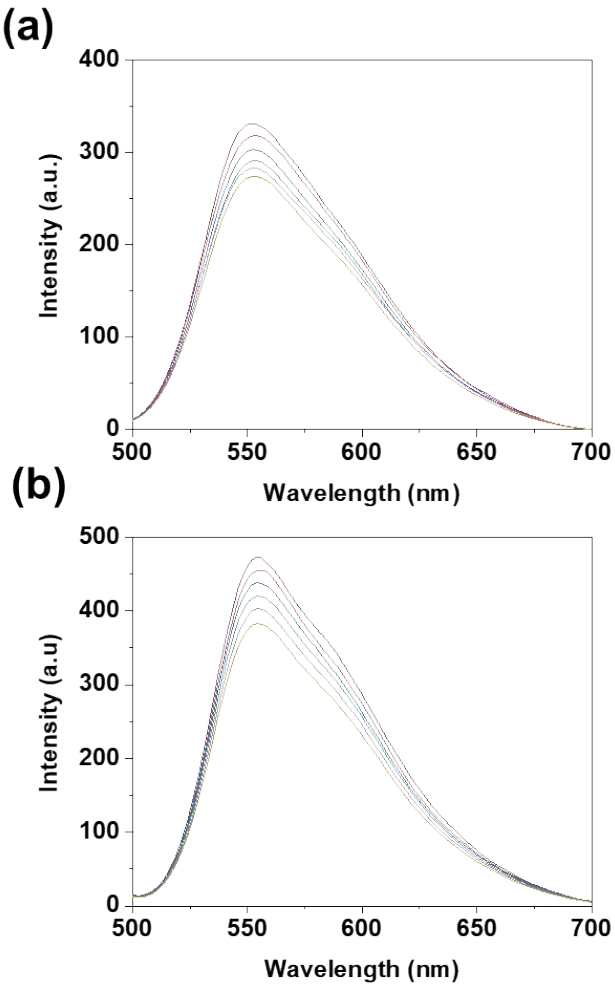

Fig. S8 Fluorescence spectra of (a) TTTT-COF-1 and (b) TTTT-COF-2 with different DNP concentration.

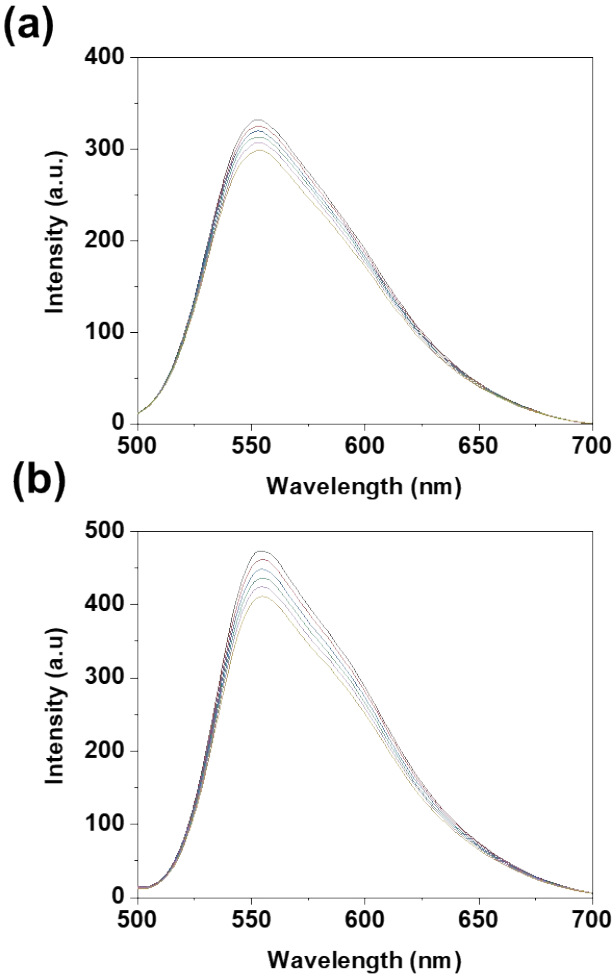

Fig. S9 Fluorescence spectra of (a) TTTT-COF-1 and (b) TTTT-COF-2 with different DNT concentration.

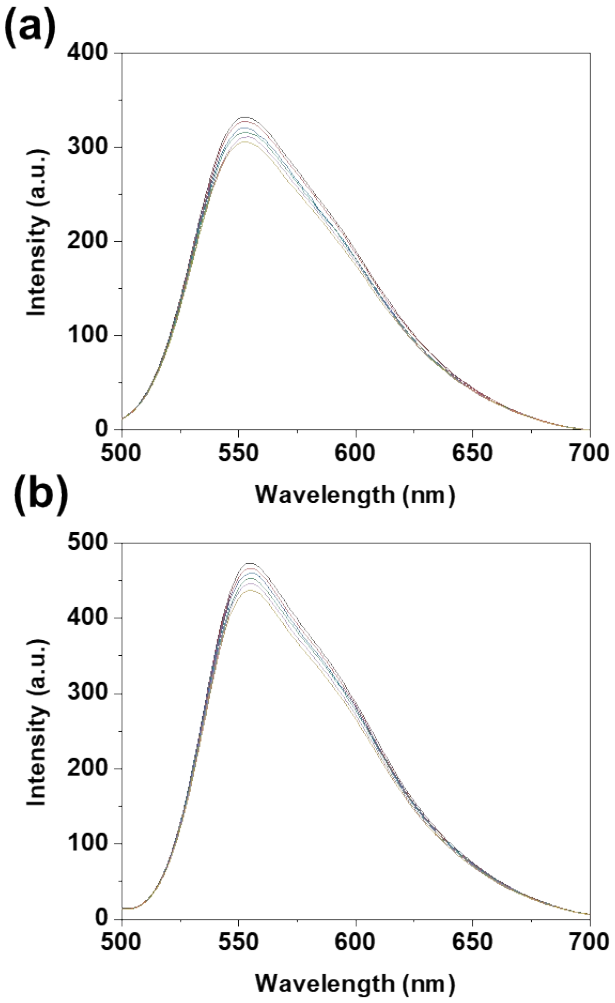

Fig. S10 Fluorescence spectra of (a) TTTT-COF-1 and (b) TTTT-COF-2 with different NP concentration.

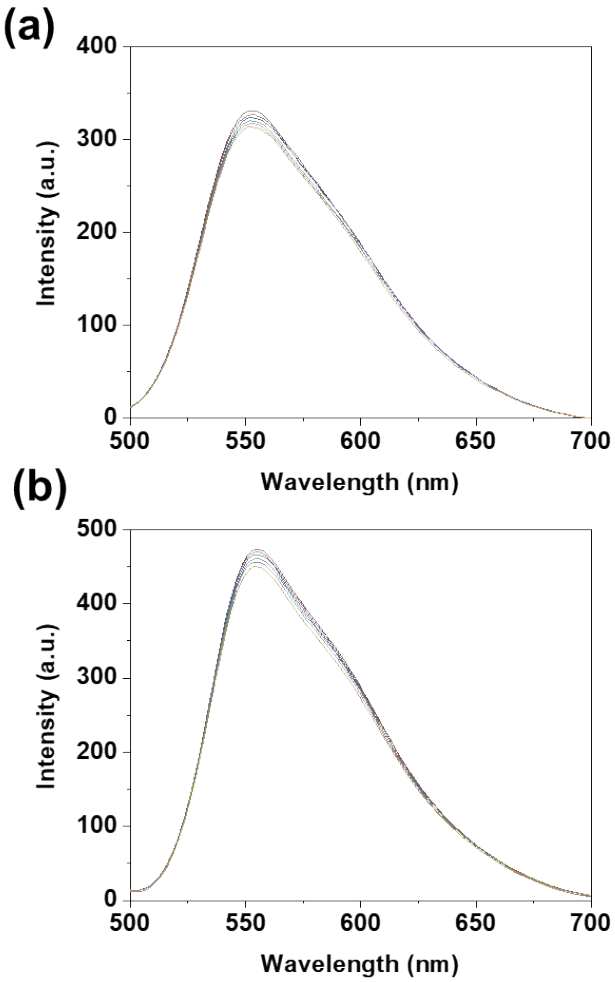

Fig. S11 Fluorescence spectra of (a) TTTT-COF-1 and (b) TTTT-COF-2 with different NT concentration.

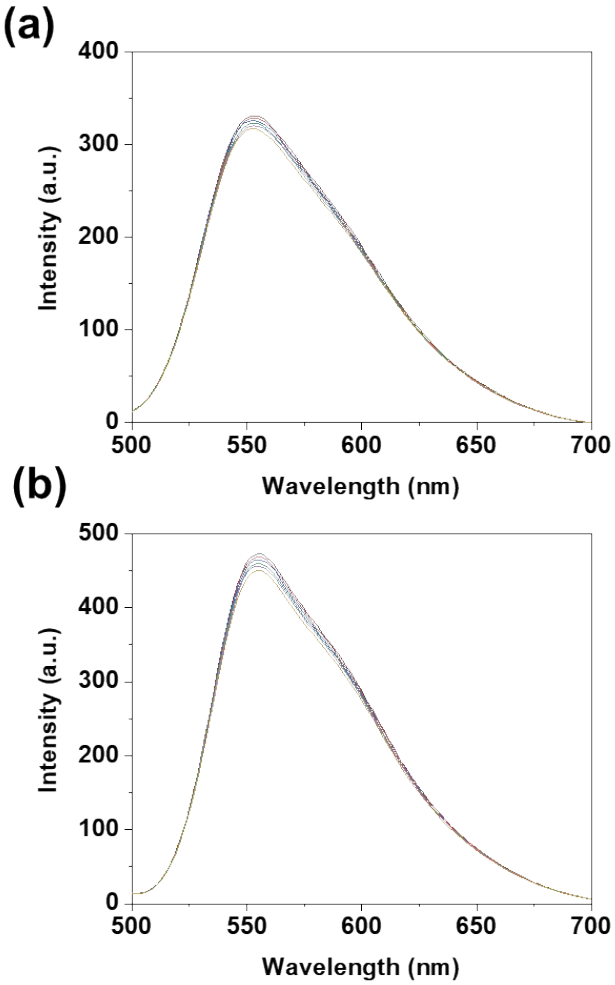

Fig. S12 Fluorescence spectra of (a) TTTT-COF-1 and (b) TTTT-COF-2 with different NB concentration.

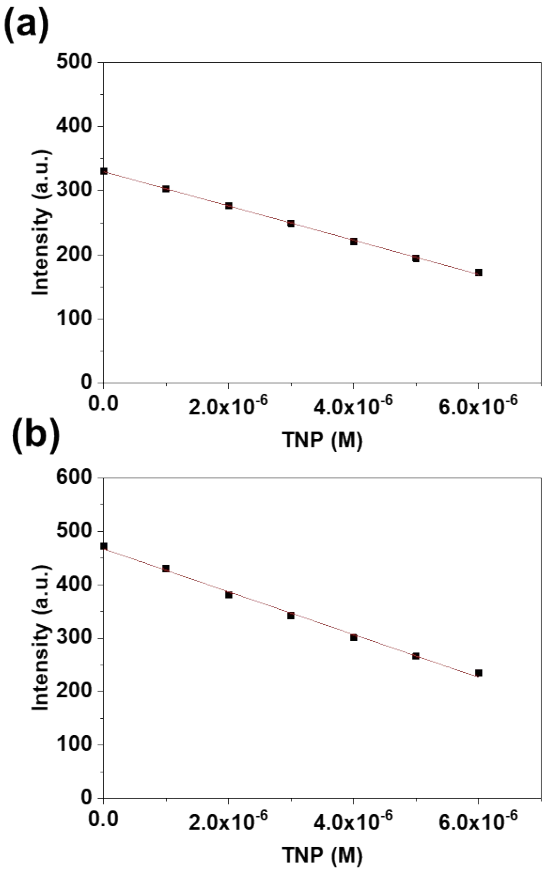

Fig. S13 PL quenching Intensity of (a) TTTT-COF-1 and (b) TTTT-COF-2 as a function of TNP concentration.

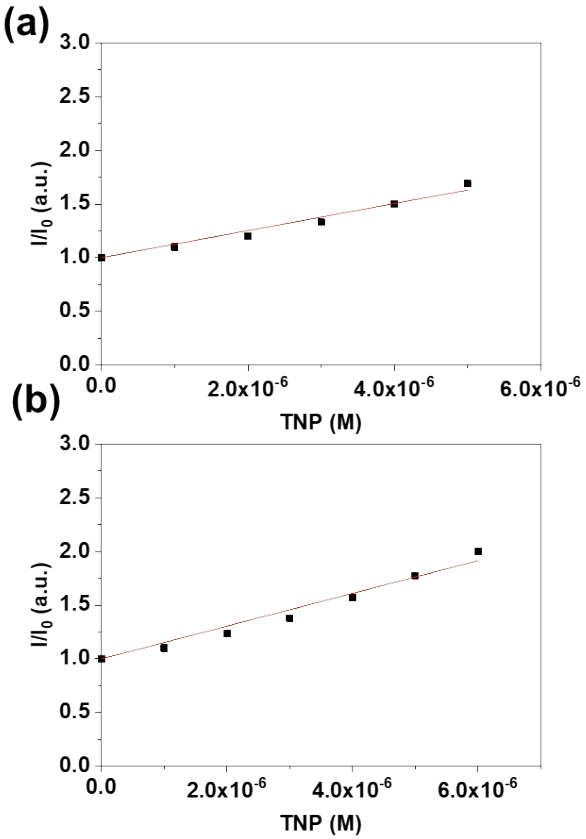

Fig. S14 Plot of PL quenching efficiency (I_0/I) of (a) TTTT-COF-1 and (b) TTTT-COF-2 as a function of TNP concentration.

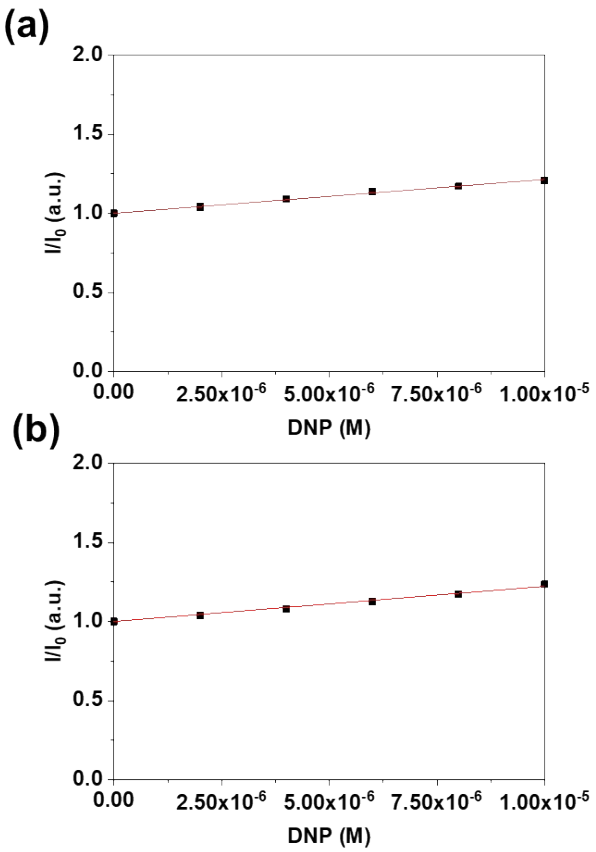

Fig. S15 Plot of PL quenching efficiency (I_0/I) of (a) TTTT-COF-1 and (b) TTTT-COF-2 as a function of DNP concentration.

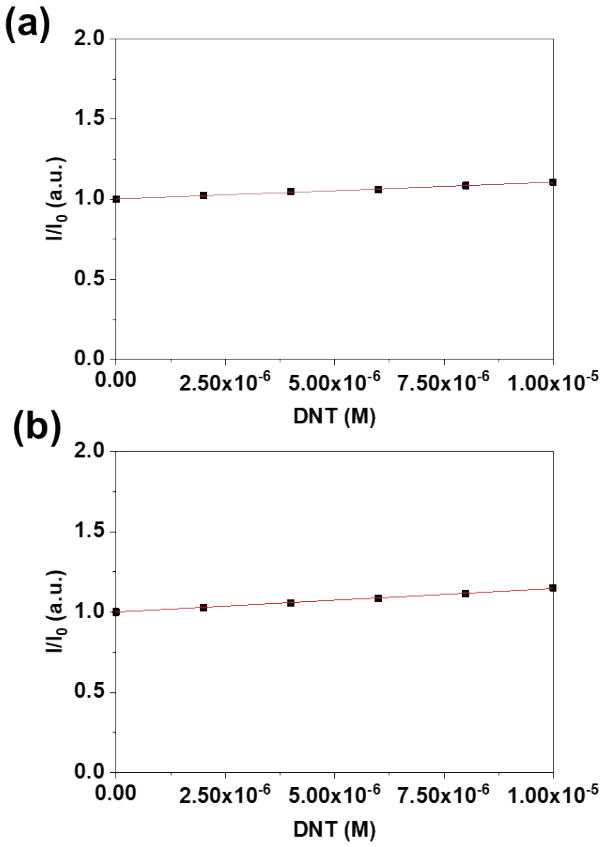

Fig. S16 Plot of PL quenching efficiency (I_0/I) of (a) TTTT-COF-1 and (b) TTTT-COF-2 as a function of DNT concentration.

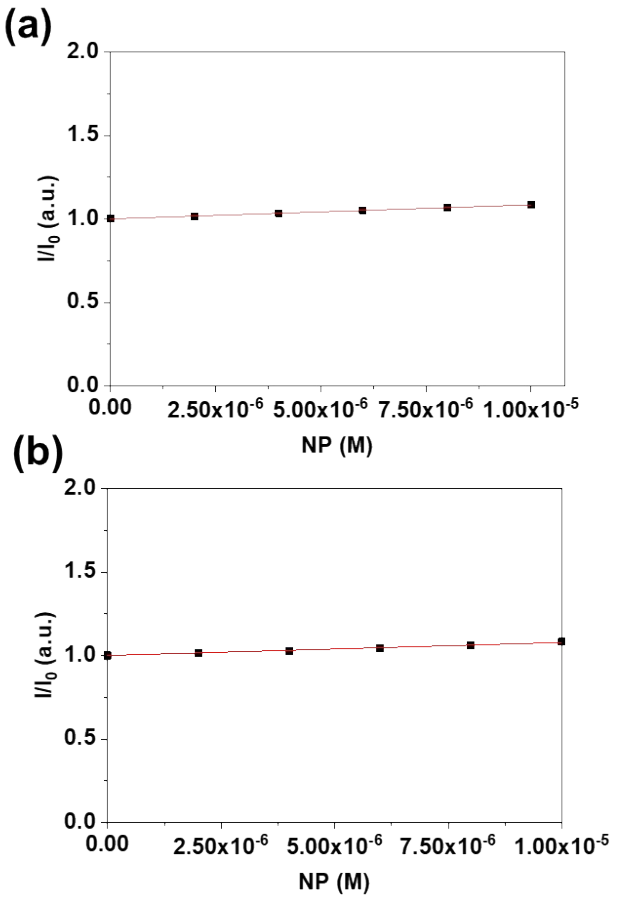

Fig. S17 Plot of PL quenching efficiency (I_0/I) of (a) TTTT-COF-1 and (b) TTTT-COF-2 as a function of NP concentration.

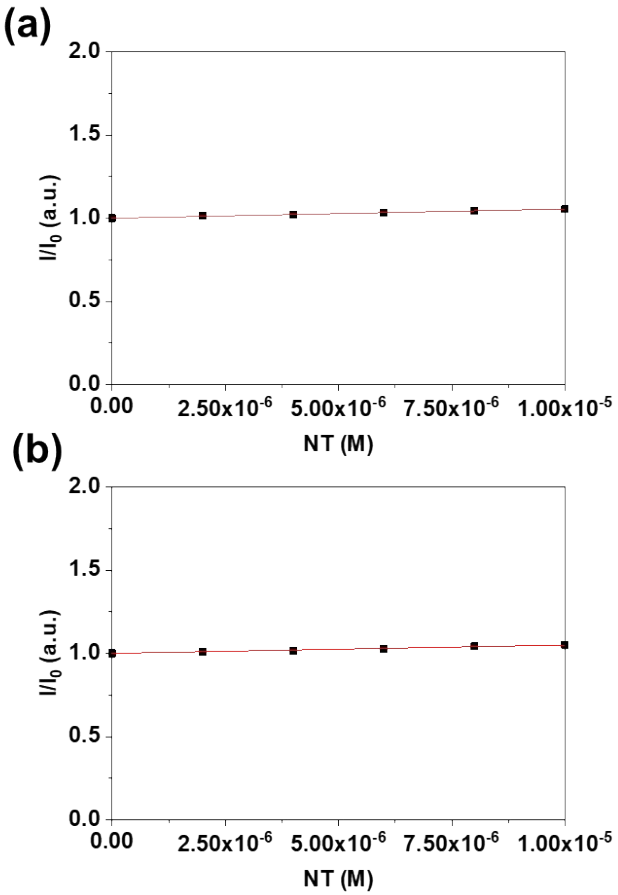

Fig. S18 Plot of PL quenching efficiency (I_0/I) of (a) TTTT-COF-1 and (b) TTTT-COF-2 as a function of NT concentration.

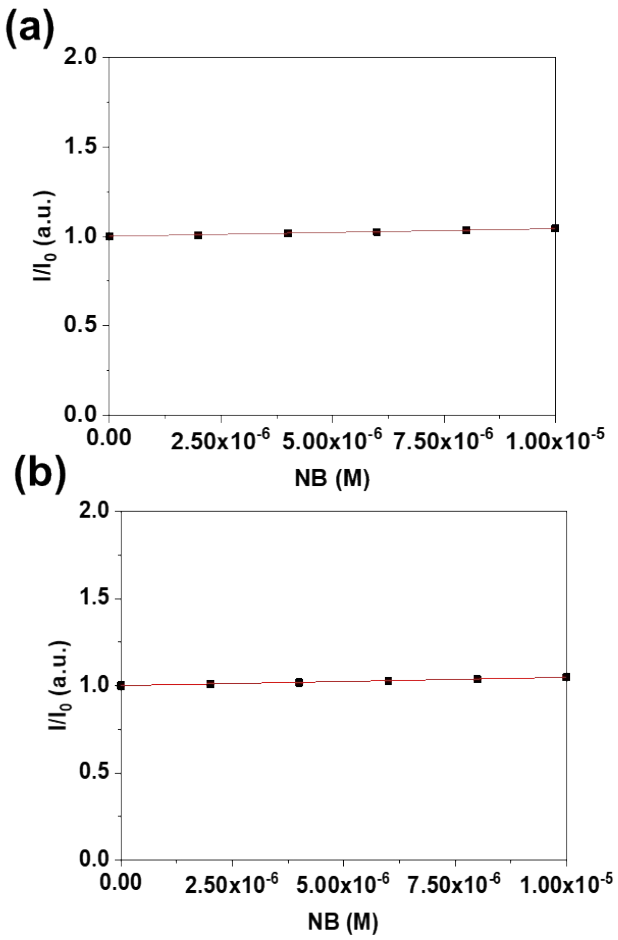

Fig. S19 Plot of PL quenching efficiency (I_0/I) of (a) TTTT-COF-1 and (b) TTTT-COF-2 as a function of NB concentration.